Coherent periodic activity in excitatory Erdös-Renyi neural networks: The role of network connectivity

Lorenzo Tattini, Simona Olmi, and Alessandro Torcini

Related Articles

Dependence of chaotic diffusion on the size and position of holes
Chaos 22, 023132 (2012)

Moments of the transmission eigenvalues, proper delay times and random matrix theory II
J. Math. Phys. 53, 053504 (2012)

On the completely integrable case of the Rössler system
J. Math. Phys. 53, 052701 (2012)

Generalized complexity measures and chaotic maps
Chaos 22, 023118 (2012)

On finite-size Lyapunov exponents in multiscale systems
Chaos 22, 023115 (2012)

Additional information on Chaos

Coherent periodic activity in excitatory Erdös-Renyi neural networks: The role of network connectivity

Lorenzo Tattini,[1,a)] Simona Olmi,[1,2,b)] and Alessandro Torcini[1,2,c)]

[1]*CNR—Consiglio Nazionale delle Ricerche—Istituto dei Sistemi Complessi, via Madonna del Piano 10, I-50019 Sesto Fiorentino, Italy*
[2]*INFN—Sezione di Firenze and CSDC, via Sansone 1, 50019 Sesto Fiorentino, Italy*

In this article, we investigate the role of connectivity in promoting coherent activity in excitatory neural networks. In particular, we would like to understand if the onset of collective oscillations can be related to a minimal average connectivity and how this critical connectivity depends on the number of neurons in the networks. For these purposes, we consider an excitatory random network of leaky integrate-and-fire pulse coupled neurons. The neurons are connected as in a directed Erdös-Renyi graph with average connectivity $\langle k \rangle$ scaling as a power law with the number of neurons in the network. The scaling is controlled by a parameter γ, which allows to pass from massively connected to sparse networks and therefore to modify the topology of the system. At a macroscopic level, we observe two distinct dynamical phases: an asynchronous state corresponding to a desynchronized dynamics of the neurons and a regime of partial synchronization (PS) associated with a coherent periodic activity of the network. At low connectivity, the system is in an asynchronous state, while PS emerges above a certain critical average connectivity $\langle k \rangle_c$. For sufficiently large networks, $\langle k \rangle_c$ saturates to a constant value suggesting that a minimal average connectivity is sufficient to observe coherent activity in systems of any size irrespectively of the kind of considered network: sparse or massively connected. However, this value depends on the nature of the synapses: reliable or unreliable. For unreliable synapses, the critical value required to observe the onset of macroscopic behaviors is noticeably smaller than for reliable synaptic transmission. Due to the disorder present in the system, for finite number of neurons we have inhomogeneities in the neuronal behaviors, inducing a weak form of chaos, which vanishes in the thermodynamic limit. In such a limit, the disordered systems exhibit regular (non chaotic) dynamics and their properties correspond to that of a homogeneous fully connected network for any γ-value. Apart for the peculiar exception of sparse networks, which remain intrinsically inhomogeneous at any system size. © 2012 American Institute of Physics. [http://dx.doi.org/10.1063/1.4723839]

The spontaneous emergence of collective dynamical behaviours in random networks made of many (identical) interacting units is a subject of interest in many different research fields ranging from biological oscillators to power grids. In particular, how the macroscopic dynamics of the network is influenced by the topology is an active research line not only for nonlinear dynamics but also for many other scientific disciplines, as for example (computational) neuroscience.[12] However, the most part of the performed analysis have been devoted to the emergence of the fully synchronized regimes, but in neuroscience a complete synchronization is usually a symptom of neural disorders, while coherent oscillations are often associated to a partial synchronization (PS) among neurons during brain activity.[8] Coherent oscillatory activities are prominent in the cortex of the awake brain during attention, and have been implicated in higher level processes, such as sensory binding, storage of memories, and even consciousness.

In this article, we analyze how the presence of disorder in the connections can influence the emergence of coherent periodic activity in Erdös-Renyi networks of excitatory pulse coupled spiking neurons. Our main result indicates that the parameter controlling the transition from asynchronous to coherent neural activity is simply the average connectivity. Furthermore, for (sufficiently large) networks the critical value of the average connectivity turns out to be independent of the network realization, sparse or massively connected, but it is instead influenced by the nature of the disorder, quenched or annealed.

I. INTRODUCTION

Neural collective oscillations have been observed in very many context in brain circuits, ranging from ubiquitous γ oscillations to θ rhythm in the hippocampus. The origin of these oscillations is commonly associated with the balance between excitation and inhibition in the network, while purely excitatory circuits are believed to lead to "unstructured population bursts."[8] However, recent "*ex vivo*" measurements performed on the rodent neocortex[3] and hippocampus[6] in the early stage of brain maturation reveal coherent activity

[a)]Electronic address: lorenzotattini@gmail.com.
[b)]Electronic address: simona.olmi@fi.isc.cnr.it.
[c)]Electronic address: alessandro.torcini@cnr.it.

patterns, such as *giant depolarizing potentials*. These collective oscillations emerge despite the fact that the GABA (γ-Aminobutyric acid) transmitter has essentially an excitatory effect on immature neurons.[5] Therefore, also in purely excitatory networks one can expect non trivial dynamics at a macroscopic level.

Numerical and theoretical studies of collective motions in networks of simple spiking neurons have been mainly devoted to balanced excitatory-inhibitory configurations, e.g., see Ref. 7 and references therein. Only few studies focused on coherent periodic activity in fully coupled excitatory networks of leaky integrate-and-fire (LIF) neurons. These analyses revealed a regime characterized by a PS at the population level, while the single neurons perform quasi-periodic motions.[23] It has been shown that the PS regime is quite robust to perturbations, since it survives to moderate levels of noise or dilution.[15,20]

Furthermore, in their recent study Bonifazi *et al.*[6] found that the functional connectivity of developing hippocampal networks is characterized by a truncated power-law distribution of the out-degrees with exponent $\gamma = 1.1$–1.3. This scaling has been shown to hold over one/two decades, thus not ensuring a scale-free distribution for the links over all scales, but surely indicating the presence of a large number of hub neurons, namely cells characterized by a high connectivity. At early developmental stages of the brain, GABAergic hub interneurons, performing complex excitatory/shunting inhibitory actions,[5] seem to be responsible for the orchestration of the coherent activity of hippocampal networks.[6] The relevance of hubs in rendering a neural circuit extremely hyper-excitable has also been demonstrated in simulation studies of a realistic model of the epileptic rat dentate gyrus, even in the absence of a scale-free topology.[16]

Motivated by these studies, but without attempting to reproduce the experimental results, we focus on a very preliminary question: to which extent is the macroscopic neural dynamics influenced by the average degree of connectivity of the neurons? Our specific aim is to analyze the key ingredients leading to the onset of coherent activity, as opposed to asynchronous dynamics, for different network size and topology.

Specifically, we consider the transition from an asynchronous regime to partial synchronization in the excitatory LIF pulse coupled neural networks introduced by Abbott and van Vreeswijk.[1] At variance with previous works, we study dynamical evolution on random Erdös-Renyi networks with an average connectivity growing (sub)-linearly with the network size N. In particular, we consider average connectivities scaling as $N^{2-\gamma}$, thus exhibiting the same system size dependence of connectivities associated to truncated power-law distributions with decay exponent $1 < \gamma < 2$. In the limit, $\gamma \to 1$ the massively connected network, where the connectivity is proportional to N, is recovered; while for $\gamma \to 2$ a sparse network, where the average probability to have a link between two neurons vanishes in the thermodynamic limit,[11] is retrieved. The topology of Erdös-Renyi networks is modified by varying the parameter γ in the interval [1:2], in particular as far as $\gamma \leq 2$ trees and cycles of any order are present in the network, while for $\gamma \to 1$ complete subgraphs of increasing order appear in the system.[2] In the paper, we will

study how and to which extent these topological modifications influence the macroscopic dynamics of the network, with particular emphasis on the transition from asynchronous to (partially) synchronous collective dynamics.

The paper is organized as follows: Sec. II is devoted to the introduction of the neural model and of the indicators employed to characterize the dynamics of the network. The phase diagram reporting the collective states emerging in our system is described in Sec. III. The influence of finite size effects on the coherent activity is analyzed in Sec. IV, while a characterization of the neural dynamics in term of maximal Lyapunov exponent is reported in Sec. V. A brief discussion of our results is outlined in Sec. VI.

II. MODEL AND METHODS

A. The model

We study a network of N LIF neurons with the membrane potential $x_i(t) \in [0 : 1]$ of the neuron i evolving as:

$$\dot{x}_i(t) = a - x_i(t) + I_i(t) \quad i = 1, ..., N, \tag{1}$$

where $a > 1$ is the suprathreshold DC current and I_i is the synaptic current. Whenever the neuron reaches the threshold $x_i = 1$, a pulse $s(t)$ is instantaneously transmitted to all the connected post-synaptic neurons and the membrane potential of neuron i is reset to $x_i = 0$. The synaptic current can be written as $I_i(t) = gE_i(t)$, with $g > 0$ representing the synaptic excitatory strength while the field $E_i(t)$ is the linear superposition of the pulses $s(t)$ received by neuron i in the past, in formula

$$E_i(t) = \frac{1}{k_i} \sum_{n|t_n < t} C_{j,i} \Theta(t - t_n) s(t - t_n), \tag{2}$$

where k_i is the number of pre-synaptic neurons connected to the neuron i (i.e., the in-degree of neuron i) and $\Theta(t)$ is the Heaviside function. The connectivity matrix $C_{j,i}$ appearing in Eq. (2) has entry 1 (respectively 0) depending if the pre-synaptic firing neuron j is connected (respectively not connected) to neuron i and in general it is not symmetric.

Following van Vreeswijk[23] we assume, for the single pulse emitted at $t = 0$, the shape $s(t) = \alpha^2 t \exp(-\alpha t)$. The explicit equation (2) can be thus rewritten as an implicit ordinary differential equation:

$$\ddot{E}_i(t) + 2\alpha \dot{E}_i(t) + \alpha^2 E_i(t) = \frac{\alpha^2}{k_i} \sum_{n|t_n < t} C_{j,i} \delta(t - t_n). \tag{3}$$

The continuous time evolution of the network can be transformed in a discrete time event-driven map by integrating Eq. (3) from time t_n to time t_{n+1}, t_n being the time immediately after the n-th spike emission.

Following Olmi *et al.*,[20] the event-driven map read as:

$$E_i(n + 1) = E_i(n)e^{-\alpha\tau(n)} + Q_i(n)\tau(n)e^{-\alpha\tau(n)} \tag{4}$$

$$Q_i(n + 1) = Q_i(n)e^{-\alpha\tau(n)} + C_{m,i}\frac{\alpha^2}{k_i} \tag{5}$$

$$x_i(n + 1) = x_i(n)e^{-\tau(n)} + a(1 - e^{-\tau(n)}) + gH_i(n), \quad (6)$$

where $Q_i \equiv \alpha E_i + \dot{E}_i$ is an auxiliary variable and $\tau(n) = t_{n+1} - t_n$ is the inter-spike time interval. This can be determined by solving the following implicit relationship

$$\tau(n) = \ln\left[\frac{a - x_m(n)}{a + gH_m(n) - 1}\right], \quad (7)$$

where m identifies the neuron which will fire next at time t_{n+1} by reaching the threshold value $x_m = 1$.

The explicit expression for the nonlinear function $H_i(n)$ appearing in Eq. (6) is

$$H_i(n) = \frac{e^{-\tau(n)} - e^{-\alpha\tau(n)}}{\alpha - 1}\left(E_i(n) + \frac{Q_i(n)}{\alpha - 1}\right)$$
$$- \frac{\tau(n)e^{-\alpha\tau(n)}}{(\alpha - 1)}Q_i(n); \quad (8)$$

for the parameter values considered in this paper ($g > 0$ and $a > 1$), $H_i(n) > 0$.

The evolution of the system is now modeled with a discrete time map of $3N - 1$ variables, $\{E_i, Q_i, x_i\}$. In fact, the construction of the event-driven map implies that the membrane potential of the neuron firing at time t_{n+1} is always equal to the threshold value, therefore this degree of freedom does not take part to the discrete time dynamics. This procedure corresponds to perform a suitable Poincaré-section. Furthermore, the evolution of the model is performed by assuming that only one neuron at a time will reach the threshold. We have checked this assumption during the map evolution and verified that it is always fulfilled in our model with the chosen pulse shape and parameter values. The event-driven scheme here described should be adapted to take in account the case of more than one neuron firing together. In practice, the map evolution is performed in three steps: first the next firing neuron (denoted as m above) should be identified, this is done by evaluating the expected firing times for all the membrane potentials by employing Eq. (7) and by selecting the neuron m associated with the minimal τ value; second, the map is evolved by employing Eqs. (4)–(6); and finally, x_m is reseted to zero.

More details on the model are reported in Ref. 20; however, at variance with that study the pulse amplitudes, appearing in Eqs. (2), (3), and (5), are normalized by the in-degree k_i of neuron i and not by the total number of neurons N. The model parameters were fixed as $a = 1.3$, $g = 0.4$, and $\alpha = 9$, in order to ensure the emergence of a PS regime in the corresponding fully coupled network.[23]

B. The connectivity matrix

In order to reveal the possible influence of network topology on the dynamics of the system, we consider Erdös-Renyi random network with an average connectivity growing (sub)-linearly with N.[2] The scaling of the average connectivity with the system size is controlled by a parameter γ and in Secs. III, IV and V, we will analyze how the dynamical properties of the network are influenced by the values of this pa-

rameter, i.e., by different ways of approaching the thermodynamic limit. In particular, we consider a directed Erdös-Renyi random graph, where the distribution of links k per neuron is well approximated by a Poisson distribution,[2] namely:

$$P(k) = e^{-\langle k \rangle}\frac{\langle k \rangle^k}{k!}. \quad (9)$$

According to Eq. (9), the degree distribution is completely defined once the value of $\langle k \rangle$ is given. To make a link with recent experimental findings obtained for excitatory networks revealing power-law distributed connectivity,[6] we choose

$$\langle k \rangle = \frac{p}{2 - \gamma}[N^{2-\gamma} - 1]. \quad (10)$$

The above expression corresponds to the average connectivity associated to a truncated power-law distribution $P(k) = pk^{-\gamma}$, once assumed that each neuron has at least one connection, and where p is a proportionality factor. We limit our analysis to $1 < \gamma < 2$, since Bonifazi et al.[6] have measured quite low values for the exponent γ, namely $\gamma = 1.1$–1.3, suggesting the existence of a large number of highly connected neurons, hubs, in the network.

As a matter of fact, by choosing for $\langle k \rangle$ the expression (10), the probability of existence of an unidirectional link connecting neuron j to i (i.e., the probability to have $C_{j,i} = 1$) is:

$$Pr(N, \gamma) = \frac{\langle k \rangle}{N} = \frac{p}{2 - \gamma}\left[N^{1-\gamma} - \frac{1}{N}\right]. \quad (11)$$

In the limit $\gamma \to 1$, the massively connected network is recovered,[11] since the average connectivity $\langle k \rangle = p \times (N - 1)$ is proportional to the system size and $Pr(N, 1) = p(1 - 1/N)$ is, apart finite-size corrections, constant and coincident with p. For $\gamma < 2$ (respectively, $\gamma > 2$), the average number of synaptic inputs per neuron will grow (respectively decrease) with N, in the limiting case $\gamma = 2$ a sparse network will be essentially recovered[27] since $\langle k \rangle = p\ln N$ will vary in a limited manner with respect to the system size. Indeed, by varying N by three orders of magnitude from 100 to 100 000 the value of $\langle k \rangle$ will modify from 3.7 to 9.2 with $p = 0.8$. In the following, we study networks of various sizes N, ranging from $N = 100$ to $N = 200\,000$, for different γ-values in the interval [1:2]. The value p is usually fixed to 0.8, apart for $\gamma = 1$ (constant probability (CP) case) when p indeed coincides with the probability to have a unidirectional link. In such case, the dependence on p is examined in details in Sec. III.

Let us stress that in the present study the distributions of pre-synaptic (in-degree) and of post-synaptic (out-degree) connections are identical, and this is guaranteed by the above outlined procedure to determine unidirectional links for Erdös-Renyi networks.

In what follows, we consider two different ways to select the random connectivity matrix: in the first case, the synaptic connections are randomly chosen before the simulation and they do not change in time (*quenched disorder*); while for the

second procedure, the post-synaptic neurons receiving the emitted pulse (i.e., the efferent connections) are randomly selected each time a neuron fires (*annealed disorder*). The latter choice can be justified from a physiological point of view by the fact that the synaptic transmission of signals is an *unreliable* process.[10] It should be noticed that in the annealed case, since the network modifies in time, the pulse amplitudes are normalized by the average in-degree $\langle k \rangle$ and not by k_i as in the quenched case.

C. Characterization of macroscopic attractors

In order to perform a macroscopic characterization of the dynamical states of the network, we exploit the average fields:

$$\bar{E}(t) = \frac{g}{N} \sum_{i=1}^{N} E_i(t), \quad \bar{Q}(t) = \frac{g}{N} \sum_{i=1}^{N} Q_i(t); \quad (12)$$

where the fields have been also rescaled by the synaptic strength as done in Ref. 20.

As a measure of the level of homogeneity among the neurons of the network, we consider the standard deviation $\sigma(t)$ of the fields $\{E_i(t)\}$ acting on the single neurons

$$\sigma(t) = \left(\frac{g^2}{N} \sum_{i=1}^{N} E_i^2(t) - \bar{E}^2(t) \right)^{1/2}; \quad (13)$$

for completely homogeneous systems, such as globally coupled networks, $E_i(t) \equiv \bar{E}$ and $\sigma \equiv 0$.

The degree of synchronization among the neurons is quantified by the order parameter usually employed in the context of phase oscillators[13]

$$R(t) = \left| \frac{1}{N} \sum_{j=1}^{N} e^{i\theta_j(t)} \right|, \quad (14)$$

where θ_j is the phase of the jth neuron, which can be properly defined as a (suitably scaled) time variable,[26] $\theta_j(t) = 2\pi(t - t_{j,n})/T_{q,n}$, where $t_{j,n}$ indicates the time of the last spike emitted by the jth neuron, while $T_{q,n} = t_{q,n+1} - t_{q,n}$ is the n-th inter-spike interval associated to the neuron q which was the last to fire in the network.[28]

A non zero-value of R represents an indication of *partial* synchronization among the neurons, while a vanishingly small $R \sim 1/\sqrt{N}$ is observable for asynchronous states (ASs) in finite systems.[13]

D. Lyapunov analysis

The dynamical microscopic instabilities of a system can be characterized in terms of the maximal Lyapunov exponent λ: a positive λ being a measure of the degree of chaoticity of the considered system. In particular, the stability of Eqs. (4)–(6) can be analyzed by following the evolution of infinitesimal perturbations in the tangent space. The corresponding equations are obtained by linearizing (4) as follows,

$$\delta E_i(n+1) = e^{-\alpha\tau(n)}[\delta E_i(n) + \tau(n)\delta Q_i(n)]$$
$$- e^{-\alpha\tau(n)}[\alpha E_i(n) + (\alpha\tau(n)-1)Q_i(n)]\delta\tau(n), \quad (15a)$$

$$\delta Q_i(n+1) = e^{-\alpha\tau(n)}[\delta Q_i(n) - \alpha Q_i(n)\delta\tau(n)], \quad (15b)$$

$$\delta x_i(n+1) = e^{-\tau(n)}[\delta x_i(n) + (a - x_i(n))\delta\tau(n)]$$
$$+ g\delta H_i(n) \quad i = 1, ..., N; \quad \delta x_m(n+1) \equiv 0; \quad (15c)$$

where the condition $\delta x_m(n+1) \equiv 0$ is due to the Poincaré map we are implementing to evolve the network dynamics.

An explicit expression of $\delta\tau(n)$ can be obtained by differentiating Eqs. (7) and (8)

$$\delta\tau(n) = \tau_x \delta x_m(n) + \tau_E \delta E_m(n) + \tau_Q \delta Q_m(n), \quad (16)$$

where

$$\tau_x := \frac{\partial\tau}{\partial x_m}, \quad \tau_E := \frac{\partial\tau}{\partial E_m}, \quad \tau_Q := \frac{\partial\tau}{\partial Q_m}. \quad (17)$$

Moreover, $\delta H_i(n)$ is a short-cut notation for the linearization of expression (8), which in turn depends on $\delta E_i(n), \delta Q_i(n)$, and $\delta\tau(n)$. For more mathematical details see Ref. 25.

To estimate the maximal Lyapunov exponent λ, we follow the usual procedure,[22] in particular, we measure the exponential growth rate of an infinitesimal perturbation by iterating the system (15). In order not to loose accuracy in the estimation, the amplitude of the perturbation should be rescaled at regular intervals, in our case we have rescaled every 1000 spikes.

The method here outlined to estimate the maximal Lyapunov exponent originates from a methodology previously introduced for continuous time dynamics interrupted by discontinuous events occurring at discrete times.[17,18] In particular, our approach differentiates from previous applications of the latter method to non-smooth flux associated to spiking neuronal models,[9,24] because we consider the evolution in the tangent space associated to a suitable Poincaré map connecting successive events.

III. PHASE DIAGRAM

In this model, two different macroscopic regimes can be observed: the asynchronous state and the partial synchronization. The asynchronous state is characterized by an incoherent dynamics of the neurons in the network leading to a spot-like macroscopic attractor in the $(\bar{E}, \bar{Q})$ plane and an almost constant average field $\bar{E}$,[1] while to the coherent PS regime corresponds a closed curve attractor[15] and a periodic behavior of $\bar{E}$ in time as shown in Figs. 1(a) and 1(b). The incoherent and coherent neural dynamics can be clearly appreciated, in the two regimes, also at microscopic level by examining the corresponding raster plots reported in Figs. 1(c) and 1(d).

As a first aspect, we will investigate the occurrence of asynchronous and partially synchronized states for finite networks and different average connectivity $\langle k \rangle$. In order to distinguish the two regimes, we have examined the macroscopic
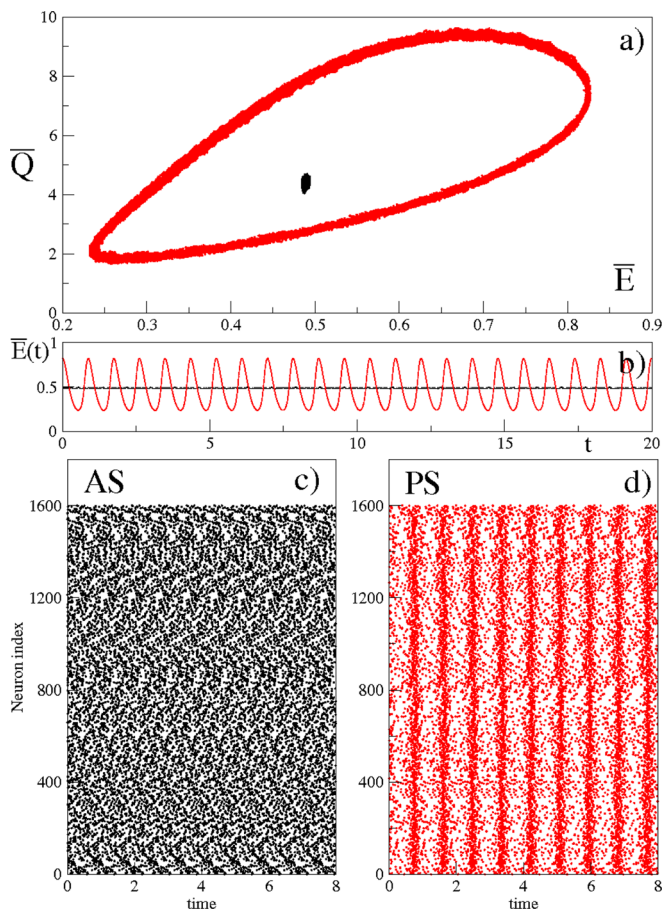
FIG. 1. Characterization of the AS and of the PS one in terms of macroscopic fields and single neuron dynamics. Panel (a): macroscopic attractors in the $(\bar{E}, \bar{Q})$ plane. Panel (b): the average field $\bar{E}$ as a function of time. Panels (c) and (d): raster plots. The data refer to Erdös-Renyi networks with $\langle k \rangle = p \times N$, quenched disorder, and $N = 1600$, the black (respectively, red) symbols correspond to the asynchronous state observable for $p = 0.2$ (respectively, PS for $p = 0.7$).

attractor shape, the extrema values of the average field $\bar{E}$, and the synchronization parameter R as a function of N.

A. Erdös-Renyi networks with constant probability

As an initial reference study, we consider Erdös-Renyi networks with unidirectional links chosen at random with a constant probability p for any network size N. This amounts to consider the limiting case $\gamma \rightarrow 1$ and to have an average connectivity scaling linearly with the size, i.e., $\langle k \rangle = pN$. Let us first examine the minima and maxima of $\bar{E}$ of a network of size N by varying the probability p between 0 and 1, as shown in Fig. 2(a) for $N = 1600$. At low probability, one has an asynchronous state while the PS regime emerges only for sufficiently large p, both in the quenched and annealed case. This result is related to the fact that the presence of noise or disorder reduces the coherence needed to observe the PS regime.[15] As a matter of fact increasing p (i.e., diminishing the number of broken links in the network) the attractor size increases and finally reaches the fully coupled result. The degree of coherence can be measured in terms of the average synchronization indicator $\langle R \rangle$. As shown in Fig. 2(b), the system coherence steadily increases with p, except in the
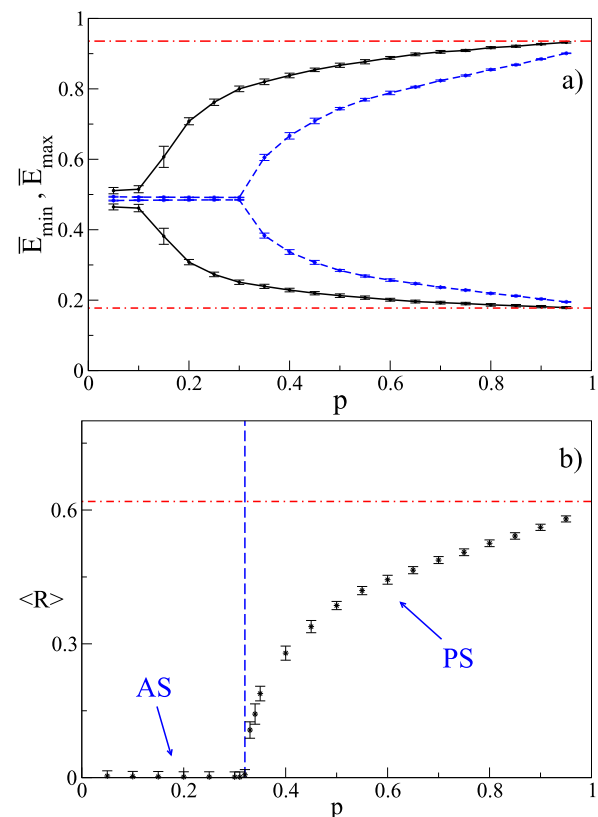

FIG. 2. (a) Minima and maxima of the average field $\bar{E}$ as a function of p, the circles joined by solid lines refer to the annealed disorder, while the stars connected by the dashed line to the quenched case. The dotted-dashed (red) lines indicate the fully coupled results (corresponding to $p \equiv 1$). (b) Synchronization indicator $\langle R \rangle$ averaged over time as a function of p for the quenched case. The data refer to Erdös-Renyi networks with CP and size $N = 1600$ and have been estimated, after discarding a transient of 4×10^7 spikes, by averaging over a train of 1–2×10^7 spikes.

asynchronous regime, where $\langle R \rangle \sim 0$, apart for finite size fluctuations.

Let us now report the phase diagram for the macroscopic activity of the network in the $(N, \langle k \rangle)$ plane, for both annealed and quenched disorder. Increasing the average connectivity, keeping the system size fixed, leads to a transition from asynchronous to partially synchronized regimes (see Fig. 3). The transition occurs at a critical average connectivity $\langle k \rangle_c$, indicates by the asterisks connected by a black solid line in Fig. 3, which for low N increases steadily with N, but eventually saturates for $N > 10\,000$ to an asymptotically constant value which depends on the disorder realization: namely, $\langle k \rangle_{as} = 725 \pm 25$ for the quenched case and $\langle k \rangle_{as} = 225 \pm 25$ in the annealed one.[29]

B. Erdös-Renyi networks with γ-dependent probability

To verify the generality of these results, we investigate Erdös-Renyi networks with γ-dependent probability. In particular, we have estimated, for system sizes in the range $100 < N < 200\,000$, the macroscopic attractors for various γ-values (namely, $\gamma = 1.1$, 1.3, 1.5, and 1.7), after discarding long transient periods. For small system sizes, the network is in the asynchronous regime which is characterized by a spot-like attractor in the $(\bar{E}, \bar{Q})$-plane. For larger number of
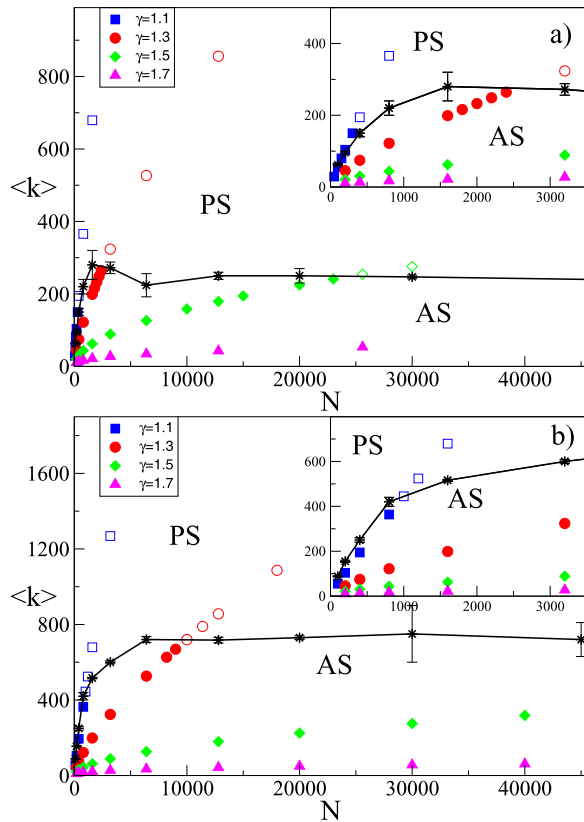
FIG. 3. Phase diagram for the macroscopic activity of the network in the $(N, \langle k \rangle)$ plane: (a) annealed disorder and (b) quenched disorder. The (black) asterisks connected by the solid (black) line correspond to the transition values $\langle k \rangle_c$ from AS to PS regime estimated for Erdös-Renyi networks with constant probability. The other symbols refer to Erdös-Renyi with $\gamma > 1$: solid (respectively, empty) symbols individuate asynchronous (respectively, partially synchronized) states. In particular, (blue) squares refer to $\gamma = 1.1$, (red) circles to $\gamma = 1.3$, (green) diamonds to $\gamma = 1.5$, and (magenta) triangles to $\gamma = 1.7$. The reported data are relative to the state of the network after discarding transients ranging from 2×10^7 spikes at the smaller sizes to 3×10^8 spikes for the larger networks.

neurons, PS emerges in the system characterized by closed curve (macroscopic) attractors. Furthermore, similarly to the results reported in Ref. 20, increasing N the curves tend to an asymptotic shape, corresponding to the fully coupled attractor, while fluctuations diminish. To exemplify this point, various macroscopic attractors for $\gamma = 1.3$ and annealed disorder are reported in Fig. 4(a).

As already reported for the constant probability networks, the systems with annealed disorder converge more rapidly with N towards the asymptotic fully coupled attractor with respect to the quenched case, as shown in Fig. 4(b) for $\gamma = 1.1$, 1.3, and 1.5. Increasing γ, we observe that the transition from the asynchronous to the partially synchronized regime occurs at larger and larger system size, both for annealed and quenched disorder. The results for $\gamma = 1.7$ are not shown in Fig. 4(b), since for all the examined network sizes (up to $N = 200\,000$) $\bar{E}$ extrema coincide within the error bar, indicating that the system is in the asynchronous regime.[30]

Asynchronous (respectively, partially synchronized) regimes are reported in the phase diagram displayed in Fig. 3 as filled (respectively, empty) symbols for the investigated
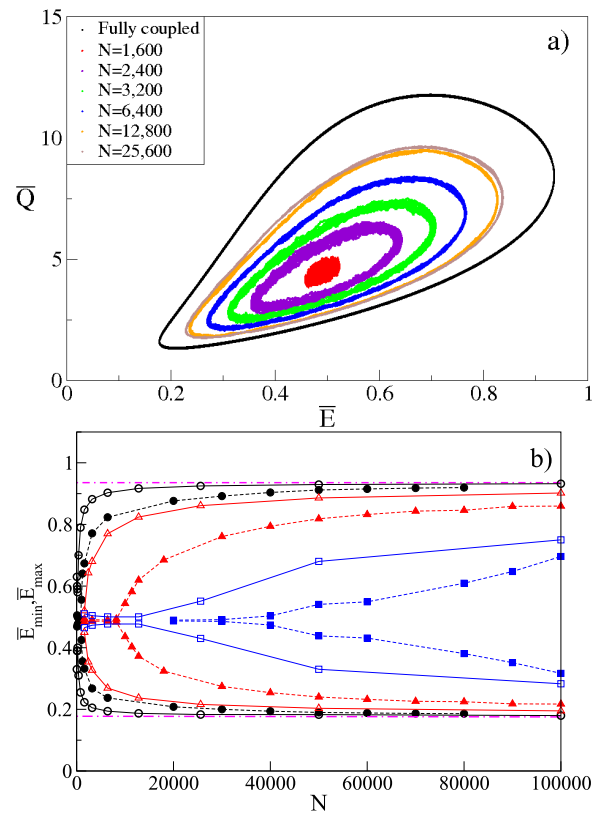

FIG. 4. (a) Macroscopic attractors in the $(\bar{E}, \bar{Q})$ plane for an Erdös-Renyi networks with $\gamma = 1.3$ and annealed disorder, the curves from the interior to the exterior correspond to increasing system sizes, from $N = 1600$ to $25\,600$. The most external (black) curve refers to a fully coupled network with $N = 3200$. (b) Minima and maxima values of the average field $\bar{E}$ as a function of N for various γ-values: namely, (black) circles $\gamma = 1.1$, (red) triangles $\gamma = 1.3$, and (blue) squares $\gamma = 1.5$. The empty (respectively, filled) symbols refer to annealed (respectively, quenched) disorder. The dotted-dashed (magenta) lines indicate the fully coupled values.

γ-values. The critical line $\langle k \rangle_c = \langle k \rangle_c(N)$ (indicated by the solid black line in Fig. 3) denoting the transition from asynchronous to partially synchronized regime coincides with that determined previously for constant probability networks. We can thus safely affirm that the dynamical regimes of the Erdös-Renyi networks depend, at a macroscopic level, simply on the average connectivity, once the system size N is fixed. This could be expected from the fact that for Erdös-Renyi networks the distribution of links per neuron is completely determined by $\langle k \rangle$ (see Eq. (9)). However, the independence of $\langle k \rangle_c$ from N at $N > 10\,000$ is unexpected and suggests that coherent behaviors, like PS regimes, can be observed in networks of any size for vanishingly small relative connectivity $\langle k \rangle / N$.

IV. NETWORK HOMOGENEITY

We observe that for any considered γ, the fields (E_i, Q_i) associated with the different neurons tend to synchronize for increasing N. Therefore, in the thermodynamic limit $(N \rightarrow \infty)$ disordered networks tend to behave as fully coupled ones, where all the neurons are equivalent and a single field is sufficient to describe the macroscopic evolution of the system.

In order to quantify the level of homogeneity among the various neurons, we measured the standard deviation

(Eq. (13)) relative to the fluctuations of the different local fields E_i with respect to the average field $\bar{E}$. In Fig. 5(a), we plot the time average of the standard deviation, $\langle\sigma\rangle$, for annealed disorder and various γ values. We observe a power law decay $\langle\sigma\rangle \propto N^{-\beta}$, where the exponent β depends on the γ-parameter as $\beta = 1 - \gamma/2$ (see Fig. 5(b)). Furthermore, for the limiting case $\gamma = 2.0$, the decay of $\langle\sigma\rangle$ is consistent with a scaling $1/\sqrt{\ln N}$ as displayed in the inset of Fig. 5(a). Altogether, the reported dependencies suggest the following relationship to hold:

$$\langle\sigma\rangle \propto \frac{1}{\sqrt{\langle k\rangle}}; \qquad (18)$$

thus, fields fluctuations are driven by the average in-degree value irrespectively of the total number of neurons. These results confirm once more that in the limit $N \to \infty$ the neural field dynamics converges to that of homogeneous networks, for both quenched and annealed disorder.

The relationship among $\langle\sigma\rangle$ and the average connectivity reported in Eq. (18) clearly indicates that for a sparse network, with constant average connectivity, $\langle\sigma\rangle$ will remain fi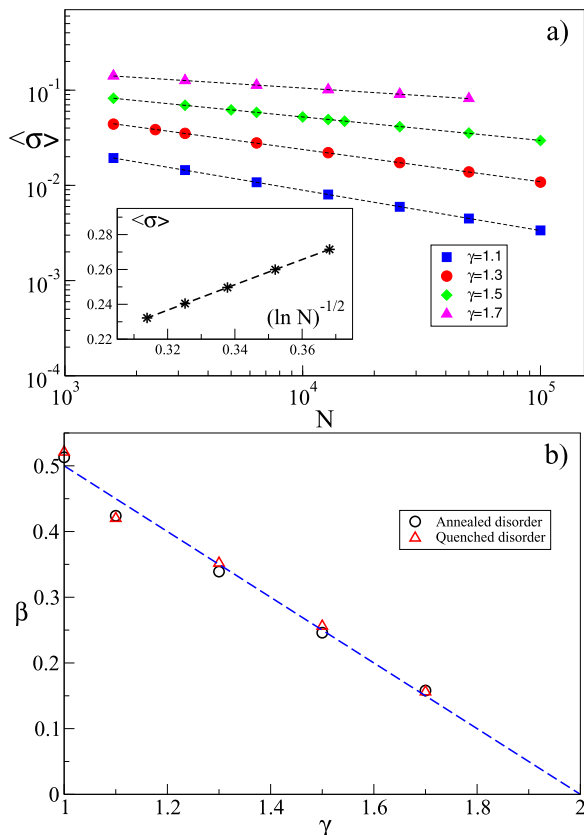nite even in the thermodynamic limit. Therefore, we can conclude that a sparse network cannot be ever reduced to a fully coupled one by simply rescaling the synaptic coupling as done in Ref. 20, even for very large systems.

V. CHAOTIC VS REGULAR DYNAMICS

Homogeneous fully connected pulse coupled networks exhibit regular dynamics.[23] In particular, for excitatory network and finite pulses the asynchronous state becomes a *splay state* characterized by all neurons spiking one after the other at regular intervals with the same frequency and by a constant mean field $\bar{E}$, while the PS regime becomes perfectly periodic at a macroscopic level.[1]

The introduction of disorder in the network leads to irregularity in the dynamics of the single neurons, which are reflected also at a macroscopic level. This kind of deterministic irregular behavior has been identified as *weak chaos* whenever the irregularity vanishes for sufficiently large system size.[19] The chaotic motion can be characterized in terms of the maximal Lyapunov exponent λ: regular orbits have non positive exponents, while chaotic dynamics are associated with $\lambda > 0$.

For finite size networks chaotic dynamics is observed both for annealed and quenched disorder. However, for all γ-values examined in this work, λ tends to decrease for a sufficiently large number of neurons in the network. Therefore, we can safely affirm that for any Erdös-Renyi network with average connectivity given by Eq. (10), the neuronal dynamics is weakly chaotic; i.e., the evolution will become completely regular for infinite networks. Numerical results for quenched disorder are reported in Fig. 6(a) for various γ-values. The maximal Lyapunov exponent exhibits clear power-law decays $N^{-\delta}$, with δ decreasing and eventually vanishing for $\gamma \to 2$ (see Table I). These results generalize previous indications reported in Olmi *et al.* for a specific realization of diluted network.[20]

Considering networks with annealed disorder it must be underlined that for sufficiently large number of neurons and $\gamma < 2$, the maximal Lyapunov reveals a tendency to decrease.

FIG. 5. (a) Average standard deviation $\langle\sigma\rangle$ versus the system size N for annealed disorder and various γ-values: $\gamma = 1.1$ (blue) squares, 1.3 (red) circles, 1.5 (green) diamonds, and 1.7 (magenta) triangles. The dashed line represents best fits with a power-law $N^{-\beta}$ to the reported data. The data in the inset (black asterisks) refer to a $\gamma = 2.0$, the dashed line is a guide for the eyes. (b) Power-law exponents β for annealed (black circles) and quenched (red triangles) disorder in the network as a function of the parameter γ. The dashed (blue) line refers to the linear law $\beta = 1 - \gamma/2$. The reported data have been estimated by averaging over trains made of 2×10^6–10^8 spikes, after discarding transients of 4×10^5–4×10^6 spikes.
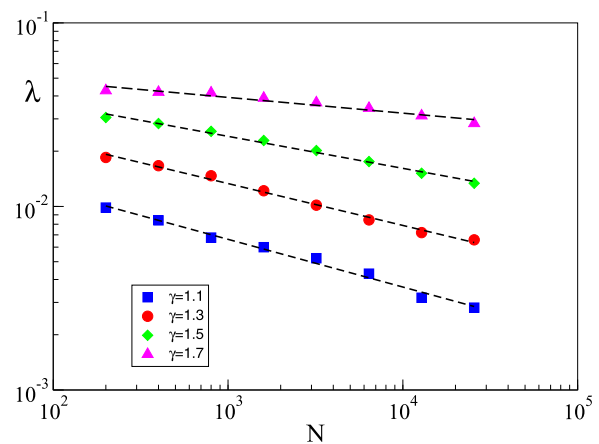

FIG. 6. Maximal Lyapunov exponents as a function of the system size N for various γ-values. The data have been obtained by discarding a transient of the order of 10^8–10^9 spikes and then by following the dynamics in the real and tangent space for an equivalent duration, moreover the data have been averaged over 3 to 5 different network realization with quenched disorder.

TABLE I. Power law exponents giving the decay of the maximal Lyapunov $\lambda \propto N^{-\delta}$ for the data reported in Fig. 6(a) for quenched disorder.

γ	δ
1.1	0.26 ± 0.01
1.3	0.228 ± 0.007
1.5	0.174 ± 0.006
1.7	0.085 ± 0.009

However, clear scaling laws cannot be inferred for all the examined γ-values on the range of affordable system sizes, namely $50 \leq N \leq 12\,500$. Larger network sizes are probably required with unreliable synapses to have clear scaling laws, due to the fact that the transition from asynchronous regime to partial synchronization occurs at critical system sizes within the investigated range. On the contrary, in the quenched case, once γ is fixed a unique regime is observable for almost all the investigated sizes. In particular, the network is always in an asynchronous regime for $\gamma = 1.7$ and 1.5, while it is in partial synchronization for $\gamma = 1.1$ and 1.3 for (almost) all the considered number of neurons. These additional findings strengthen the above reported conclusions: finite size systems are weakly chaotic for any considered dynamical regime.[31]

According to the results reported above, we expect that for sparse networks the maximal Lyapunov exponent will eventually saturate to some constant value, apart for possible logarithmic corrections. Thus, sparse networks should remain chaotic for any system size, paralleling the behavior of the microscopic fluctuations shown in Sec. IV. Therefore, microscopic inhomogeneities and chaotic behavior appear as deeply related.

VI. DISCUSSION

Collective periodic oscillations in excitatory Erdös-Renyi networks can be observed only above a critical average in-degree. This latter quantity saturates to a constant value for networks with a sufficiently large number of neurons, thus suggesting that the key ingredient responsible for the emergence of collective behaviors is the number of pre-synaptic neurons both for massively connected networks as well as for sparsely connected ones. This result confirms and generalizes previous findings on the stability of the complete synchronized state for pulse-coupled Hindmarsh-Rose neurons.[4] Furthermore, our results indicate that the minimal network size required to observe collective oscillations diverges with the exponent γ ruling the scaling of the average connectivity with the number of neurons.

The presence of annealed disorder in the network (corresponding to unreliable synapses) favors the emergence of coherent activity with respect to the quenched case (associated with reliable synapses), since in the first case the asymptotic average connectivity required to observe collective oscillations is much smaller. This is probably due to the fact that in the annealed situation each neuron is on average subjected to the same train of stimuli, while with quenched disorder the dynamics of each neuron depends heavily on its neighbors. Furthermore, for sufficiently large networks the macroscopic behavior observable with reliable or unreliable synapses becomes identical. This seems to indicate that at the level of population dynamics the reliability or unreliability in the synaptic transmission can be irrelevant.

The average in-degree $\langle k \rangle$ also controls the fluctuations among different neurons, being the fluctuations proportional to the inverse of the square root of $\langle k \rangle$. Therefore, for Erdös-Renyi networks with average in-degree proportional to any positive power of N, the fluctuations will vanish in the limit $N \to \infty$, leading to a homogeneous collective behavior analogous to that of fully connected networks. On the contrary, inhomogeneities among neurons will persist at any system size in sparse networks.

Recent experimental results on the intact neuronal network of the barrel cortex of anesthetized rats seem to clearly suggest that the dynamics of this system is chaotic.[14] This result poses severe questions about the possibility of reliable neural coding. The evolution of our models is chaotic for any finite networks. However, in the presence of coherent periodic activity, the chaoticity present in the system is not so strong to destroy the average collective motion. Thus, the trial-to-trial variability, observable in the response of each single neuron and induced by chaos, does not prevent the possibility of the network to encode information. The information can be coded in some property associated to the global (almost regular) oscillations of the network which are robust to local fluctuations emerging at the neuronal level, and this *collective coding* can represent an alternative to the dilemma rate versus spike timing coding.[14]

The level of chaos in the examined networks decreases with N and the dynamics becomes regular in the thermodynamic limit. However, the decrease of the maximal Lyapunov exponent with N slows down dramatically for $\gamma \to 2$, suggesting an erratic asymptotic behavior for sparse networks.

Our results represent only a first step in the analysis of what matters in the network topology for the emergence of coherent neural dynamics. In future works, our findings should be critically verified for more complex topologies, like scale-free and small-world, and the influence of other ingredients, like the asymmetry in the in-degree and out-degree distributions,[21] should be also addressed.

ACKNOWLEDGMENTS

[1]L. F. Abbott and C. van Vreeswijk, "Asynchronous states in networks of pulse-coupled oscillators," Phys. Rev. E **48**, 1483 (1993).

[2] R. Albert and A. L. Barabási, "Statistical mechanics of complex networks," Rev. Mod. Phys. **74**, 4797 (2002).

[3] C. Allene, A. Cattani, J. B. Ackman, P. Bonifazi, L. Aniksztejn, Y. Ben-Ari, and R. Cossart, "Sequential generation of two distinct synapse-driven network patterns in developing neocortex," J. Neurosc. **26**, 12851–12863 (2008).

[4] I. Belykh, E. de Lange, and M. Hasler, "Synchronization of bursting neurons: What matters in the network topology," Phys. Rev. Lett. **94**, 188101 (2005).

[5] Y. Ben-Ari, J. L. Gaiarsa, R. Tyzio, and R. Khazipov, "GABA: A pioneer transmitter that excites immature neurons and generates primitive oscillations," Physiol. Rev. **87**, 1215–1284 (2007).

[6] P. Bonifazi, M. Goldin, M. A. Picardo, I. Jorquera, A. Cattani, G. Bianconi, A. Represa, Y. Ben-Ari, and R. Cossart, "GABAergic hub neurons orchestrate synchrony in developing hippocampal networks," Science **326**, 1419–1424 (2009).

[7] N. Brunel, "Dynamics of sparsely connected networks of excitatory and inhibitory spiking neurons," J. Comput. Neurosci. **8**, 183 (2000).

[8] G. Buzsáki, *Rhythms of the Brain* (Oxford University Press, New York, 2006).

[9] S. Coombes, R. Thul, and K. C. A. Wedgwood, "Nonsmooth dynamics in spiking neuron models," Physica D (in press). doi: 10.1016/j.physd.2011.05.012.

[10] J. Friedrich and W. Kinzel, "Dynamics of recurrent neural networks with delayed unreliable synapses: Metastable clustering," J. Comput. Neurosci. **27**, 65 (2009).

[11] D. Golomb, D. Hansel, and G. Mato, "Mechanisms of synchrony of neural activity in large networks," in *Handbook of Biological Physics*, edited by S. Gielen and F. Moss (Elsevier, Amsterdam, 2001), pp. 887–967.

[12] G. Grinstein and R. Linsker, "Synchronous neural activity in scale-free network models versus random network models," Proc. Natl. Acad. Sci. U.S.A. **102**, 9948–9953 (2005).

[13] Y. Kuramoto, *Chemical Oscillations, Waves, and Turbulence* (Dover, 2003).

[14] M. London, A. Roth, L. Beeren, M. Häusser, and E. Latham, "Sensitivity to perturbations *in vivo* implies high noise and suggests rate coding in cortex," Nature (London) **446**, 123–128 (2010).

[15] P. K. Mohanty and A. Politi, "A new approach to partial synchronization in globally coupled rotators," J. Phys. A **39**, L415 (2006).

[16] R. J. Morgan and I. Soltesz, "Nonrandom connectivity of the epileptic dentate gyrus predicts a major role for neuronal hubs in seizures," Proc. Natl. Acad. Sci. U.S.A. **105**, 6179–6184 (2008).

[17] P. C. Müller, "Calculation of lyapunov exponents for dynamic systems with discontinuities," Chaos, Solitons Fractals **5**, 1671–1681 (1995).

[18] Ch. Dellago, H. A. Posch, W. G. Hoover, "Lyapunov instability in a system of hard disks in equilibrium and nonequilibrium steady states," Phys. Rev. E **53** (1996) 1485.

[19] O. V. Popovych, Y. L. Maistrenko, and P. A. Tass, "Phase chaos in coupled oscillators," Phys. Rev. E **71**, 065201R (2005)

[20] S. Olmi, R. Livi, A. Politi, and A. Torcini, "Collective oscillations in disordered neural networks," Phys. Rev. E **81**, 046119 (2010).

[21] A. Roxin, "The role of degree distribution in shaping the dynamics in networks of sparsely connected spiking neurons," Front. Comput. Neurosci. **5**, 8 (2011).

[22] I. Shimada and T. Nagashima, "A numerical approach to ergodic problem of dissipative dynamical systems," Prog. Theor. Phys. **61**, 1605 (1979); G. Benettin, L. Galgani, A. Giorgilli, and J. M. Strelcyn, "Lyapunov characteristic exponents for smooth dynamical systems and for hamiltonian systems; a method for computing all of them. Part II: Numerical application," Meccanica **15**, 21 (1980).

[23] C. van Vreeswijk, "Partial synchronization in populations of pulse-coupled oscillators," Phys. Rev. E **54**, 5522 (1996).

[24] D. Zhou, Y. Sun, A. V. Rangan, and D. Cai, "Spectrum of Lyapunov exponents of non-smooth dynamical systems of integrate-and-fire type," J. Comput. Neurosci. **28**, 229–245 (2010).

[25] R. Zillmer, R. Livi, A. Politi, and A. Torcini, "Stability of the splay state in pulse–coupled networks," Phys. Rev. E **76**, 046102 (2007).

[26] A. T. Winfree, *The Geometry of Biological Time* (Springer Verlag, Berlin, 1980).

[27] A sparse network is usually defined as a network where the average connectivity remains constant in the thermodynamic limit, see Ref. 11.

[28] In the original definition reported in Ref. 26, $T_{q,n} = T_{j,n}$, thus ensuring that the phase is bounded between 0 and 2π. However, this definition requires to memorize all the spiking events within a certain time interval and then estimate the phases and $R(t)$ over such time span. Our definition does not guarantee that the phase is strictly bounded within the $[0: 2\pi]$-interval, but it allows to estimate $R(t)$ during the simulation run without memorizing any event. Indeed, we have verified that, at least in the studied cases, no peculiar differences are observable by employing the two phase definitions and this is probably due to the fact that the dynamics of all the neurons in the networks are statistically equivalent.

[29] We have verified that the above reported scenario is not modified by considering fully homogeneous connectivity with $P(k) = \delta(k - k_0)$, the only difference concerns the asymptotic value $\langle k \rangle_{as}$ at which the transition from asynchronous dynamics to partial synchronization occurs. As a matter of fact, $\langle k \rangle_{as}$ is slightly smaller than for Erdös-Renyi distributions due to the absence of fluctuations among the in-degree values in the homogeneous case.

[30] A simple estimation of the minimal network size needed to observe PS for generic γ-distributions can be obtained by inverting Eq. (10) for the asymptotic values $\langle k \rangle_{as}$, namely

$$N_c = \left[\frac{p}{2 - \gamma} \langle k \rangle_{as} + 1 \right]^{1/(2-\gamma)}; \qquad (19)$$

for $\gamma = 1.7$ this leads to $N_c = 131\,784\,000$ (respectively, $N_c = 2\,740\,117$) in the quenched (respectively, annealed) case. This confirms that coherent activity is unobservable for $\gamma = 1.7$ with our computational resources for the chosen coupling parameter, namely $g = 0.4$.

[31] We have carefully verified for various system sizes that the maximal Lyapunov exponents, averaged over a suitable time window, do not vary over time and does not depend on the duration of the chosen transitory.